UCRL-JC-129721
PREPRINT

3ω Damage Threshold Evaluation of Final Optics Components using Beamlet Mule and Off-Line Testing

M. R. Kozlowski
S. Maricle
R. Mouser
S. Schwartz
P. Wegner
T. Weiland

This paper was prepared for submittal to the
Third Annual International Conference on
Solid State Lasers for Application (SSLA)
to Inertial Confinement Fusion (ICF)
Monterey, California
June 7-12, 1998

July 27, 1998

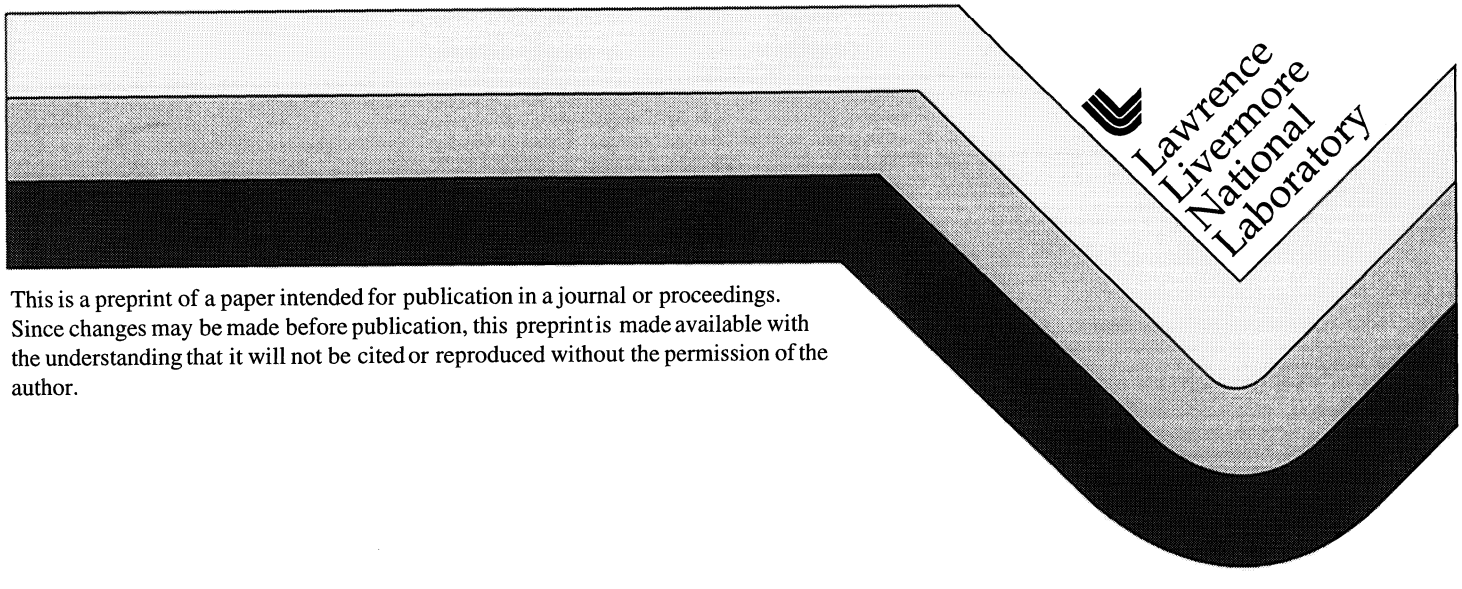

3ω Damage threshold evaluation of final optics components using Beamlet Mule and off-line testing

M.R. Kozlowski, S. Maricle, R. Mouser,
S. Schwartz, P. Wegner, T. Weiland
Lawrence Livermore National Laboratory
7000 East Avenue, Livermore, California, 94551

ABSTRACT

A statistics-based model is being developed to predict the laser-damage-limited lifetime of UV optical components on the NIF laser. In order to provide data for the model, laser damage experiments were performed on the Beamlet laser system at LLNL. An early prototype NIF focus lens was exposed to twenty 351 nm pulses at an average fluence of 5 J/cm^2, 3ns. Using a high resolution optic inspection system a total of 353 damage sites was detected within the 1160 cm^2 beam aperture. Through inspections of the lens before, after and, in some cases, during the campaign, pulse to pulse damage growth rates were measured for damage initiating both on the surface and at bulk inclusions. Growth rates as high as 79 μm/pulse (surface diameter) were observed for damage initiating at pre-existing scratches in the surface. For most damage sites on the optic, both surface and bulk, the damage growth rate was approximately 10μm/pulse.

The lens was also used in Beamlet for a subsequent 1053 μm/526 μm campaign. The 352 μm-initiated damage continued to grow during that campaign although at generally lower growth rates.

Key words: laser damage, fused silica, polishing, NIF, growth rate, defects, inclusions

1. INTRODUCTION

It is expected that under the aggressive illumination conditions of the National Ignition Facility (NIF) some laser-induced damage will occur in the fused silica optics transmitting UV laser light (351 nm or 3ω) to the target. The UV optics include the focus lens, diffractive optics plates (DOPs) and the debris shield. Combined with the KDP crystals used for frequency conversion, these optics make up the NIF final optics package. In order to evaluate the performance of final optics components, a testbed system, called the Mule, was added to the Beamlet laser system at LLNL.[1]

The goal of the experiments described here is to study the evolution of UV laser damage on a final focus lens within the Beamlet Mule. Information to be gained includes the density of damage sites on the optic and the rate of growth of the damage sites when exposed to additional laser pulses. This information will be used to develop a model for optics lifetime on the NIF laser.

Other studies have indicated that the diameter, D, of a laser damage site is fused silica grows as

$$D = N \cdot R(F) \qquad (1)$$

where N is the number of pulses and R is the growth rate in μm/pulse. R is a linear function of the fluence, F, in J/cm^2.[2] The growth rate R appears to depend on parameters such as the nature of the damage initiator, the environment of the optic (air or vacuum), and possibly the laser pulselength. In the present experiment R was to be determined at a fixed fluence for a NIF-scale focus lens (39 cm x 39 cm) in vacuum, the final optics environment in NIF.

Besides damage growth rate, the laser damage performance of an optic is determined by the density of damage initiation sites on an optic. In a paper by Feit, et al.[3] in these proceedings it is shown that the statistical nature of laser damage on surfaces can be modeled using the concepts of "extreme statistics." A methodology has been developed for predicting the density of damage sites on NIF-scale optics using data obtained by rastering an optic with 1 mm diameter gaussian laser beams. The purpose of the Beamlet Mule experiments is to provide data by which these statistical models can be evaluated.

2. DAMAGE TESTING AND OPTICS INSPECTION

2.1 Off-line testing results and inspection techniques

The tests discussed here involve two early prototype NIF reverse focus lenses 01A and 02A manufactured using ZrO_2 polishing processes. ZrO_2 polishing has been shown to result in improved laser damage performance as compared to the more common CeO_2 polishing processes.[4] Both lens was characterized before and after illumination using a Defect Mapping System (DMS). [6] This system uses fiber optic light bars to internally illuminate the optic through the four edges. A full aperture image of an optic is taken using a mega-pixel CCD camera. The system detects defects as small as 10μm over the full 40cm x 40cm optic. Due to blooming of the defects in the image, it is not possible to resolve the size or features or the individual defect/damage sites directly from the mega-pixel map. After identification of defects in the image, a long focal length microscope is used to photograph individual sites. For both lenses the majority of pre-existing surface defects were small scratches (<2mm long, <30μm wide) on the rear surface. These scratches were attributed to the use of ZrO_2 in the lens aspherization processes. Four bulk inclusions with diameters ranging from 7 to 48 μm were also observed in the lens.

Lens 01A was damage tested at 355 nm using a large-aperture raster scanning facility at LLNL (1mm diameter beam).[5] The lens was scanned at fluences ranging from 2.8 J/cm^2 to 14 J/cm^2, 3 ns, on a cumulative surface area of 80 cm^2. In those tests damage was observed at fluences as low as 2.8 J/cm^2. The damage occurred at pre-existing bulk and surface defects, as well as surface sites with no visible precursor (NVP). In those tests there was no obvious correlation indicated between damage size and precursor or fluence. Damage morphology studies using raster-scan techniques are complicated, however, by the "overlapping beam print" nature of the scanning process.

Based on the off-line tests of lens 01A, it was determined that in the Beamlet test lens 02A would be illuminated with 20 pulses at a fluence of 5 J/cm^2 average at 3ns. This fluence would provide a damage probability of <1% for 1mm^2 areas on the surface.

2.2 Beamlet Campaigns

Lens 02A was coated with a silica sol-gel anti-reflection coating before being installed in the Beamlet Mule. The Beamlet 3ω campaign included a six-pulse ramp from 0.8 to 4.3 J/cm^2 followed by twenty pulses at approximately 5 J/cm^2. The average beam modulation in the test was 1.31 to 1 (over 99.9% of area), resulting in peak fluences of approximately 7 J/cm^2. Figure 1 shows a plot of the peak and average fluences in the test. The lens was inspected inside the Mule twice during the campaign: after the first and twelfth 5 J/cm^2 pulses. Five damage sites were photographed during the inspections.

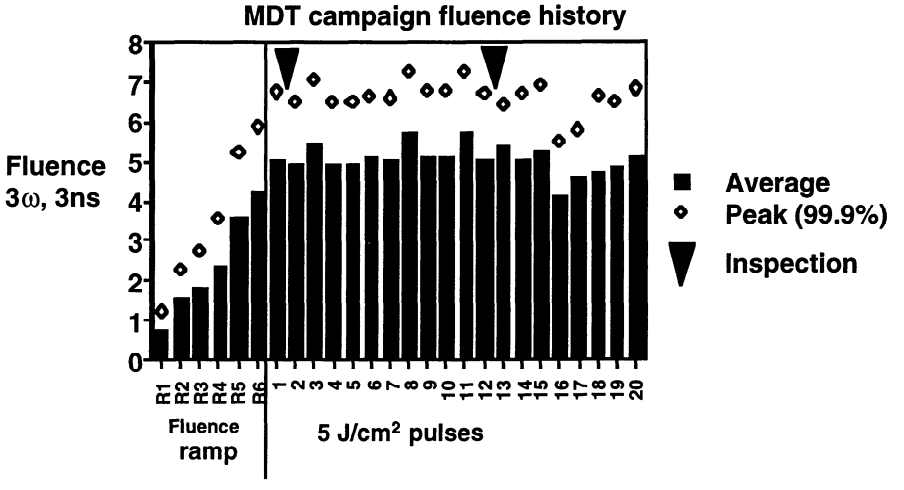

Figure 1. The 3ω campaign illuminated lens 02A with 20 pulses with an average fluence of 5.04 J/cm^2. Average modulation: 1.3.1 peak-to-average.

After the twenty shot 3ω campaign was completed the lens was removed from the Mule and mapped using the DMS system. Figure 2 shows the DMS map of the lens after the 3ω campaign. The mapping system identified 353 damage sites larger than 10 μm in diameter. As a result of camera blooming, the damage sites appear larger than they actually are. Fourteen damage sites representative of the 353 bulk and surface damage sites on the optic were further characterized using the long focal length microscope.

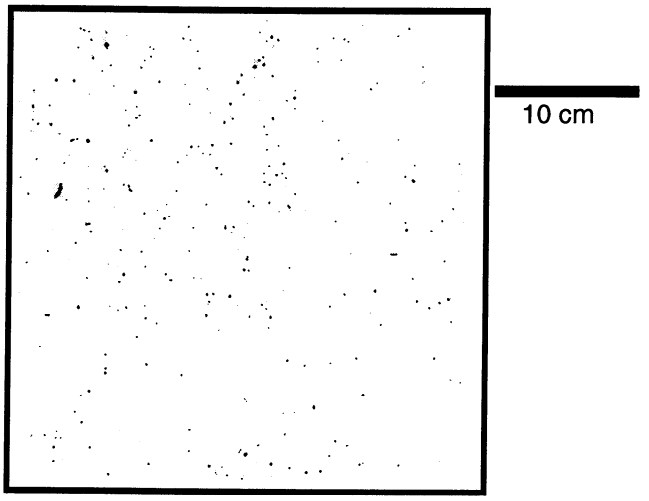

Figure 2. DMS map of lens 02A after twenty 5 J/cm^2 pulses. The map shows the location of 353 damage sites ranging in size from 10 μm to 2 mm within the 1160 cm^2 beam aperture

The lens was reinstalled on Beamlet for a series of low-fluence frequency doubling experiments. During that campaign the lens was exposed to 47 pulses of 1ω and 2ω illumination (1053 nm and 526 nm, respectively) with maximum intensities of 5.7 J/cm^2 and 4.3 J/cm^2 respectively at 1.5 ns. The mean 1ω and 2ω intensities were 2.2 J/cm^2 and 1.5 J/cm^2, respectively. Each of the fourteen sites measured after the 3ω campaign were again characterized after the 1ω/2ω campaign.

3. DAMAGE GROWTH RESULTS

3.1 3ω illumination

Damage size data obtained during the various lens inspections are shown graphically in figures 4-6. Figure 4 shows the data for the five sites characterized during the two intermediate inspections inside the Mule. The data for sites 1 and 2 support the assumption of a linear growth rate. Figure 5 shows the data for sites measured only before and after the 3ω campaign. In both figures 4 and 5 the steepest slopes (i.e. growth rates) are for preexisting scratches. The data does not indicate a clear correlation between precursor size and growth rate, consistent with the raster scan test result on lens 01A.

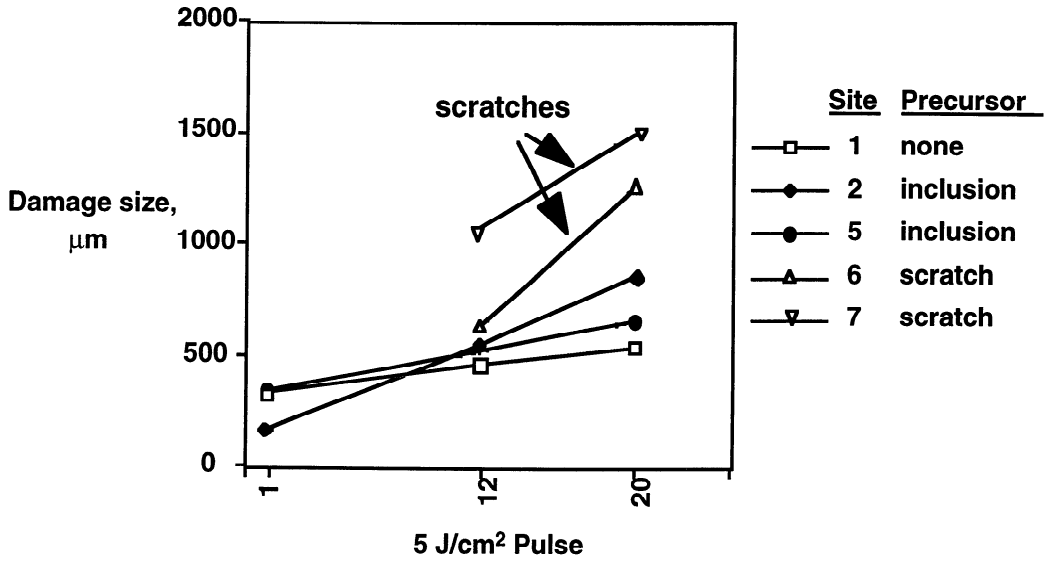

Figure 3. Damage size data for 5 rear surface sites measured during in-situ inspections. Growth rates range from 9 to 79 μm/pulse.

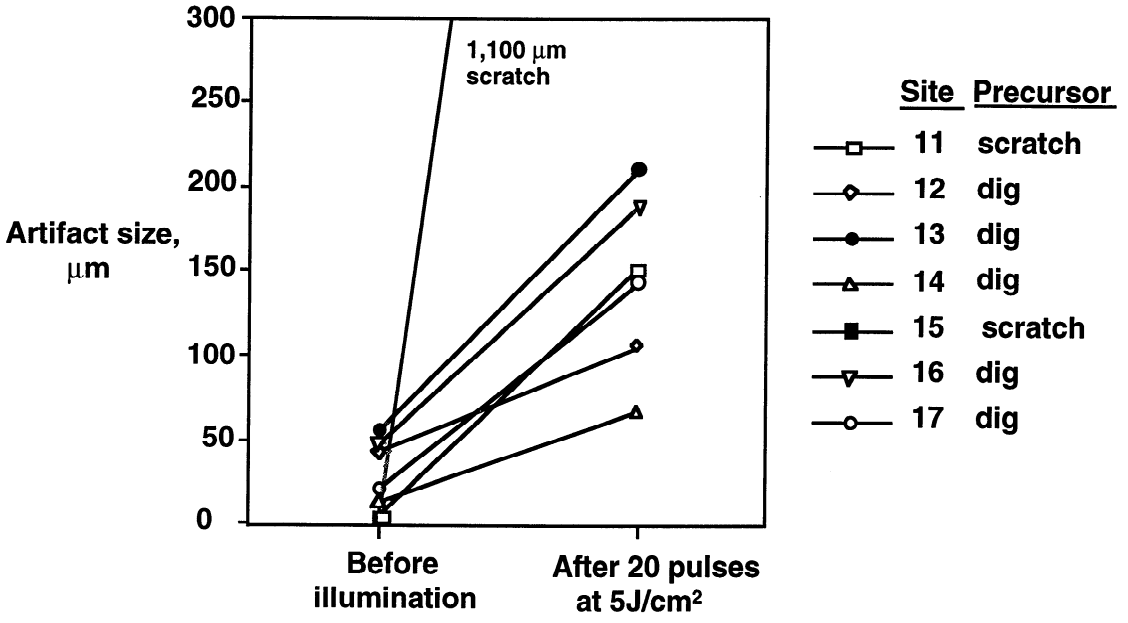

Figure 4. Sizes of damage associated with pre-existing surface defects. Growth rates range from 2.7 to 55 μm/pulse. All damage is front surface except for sites 13 and 15 (solid symbols).

Size data for damage at bulk inclusions is shown in figure 6. In figure 4, sites 2s and 5s are rear surface damage sites correlated with bulk inclusion damage. The rear surface damage is due to locally high fluences resulting from modulation of the beam by the bulk damage site.[7]

Damage growth rates were calculated from the defect/damage sizes shown in Figures 4-6 and assuming a linear growth rate. The growth rates were calculated counting only the shots at 5 J/cm^2, but not the initial six lower fluence pulses in the ramp. The influence of this simplification on the reported growth rates is small since most damage did not occur until the higher fluence shots. Damage growth rates for the 3ω campaign are summarized in figures 7 and 8, showing the dependence of the growth rate on damage precursor type (scratch, dig, inclusion, etc.) and location (bulk, input or output surface).

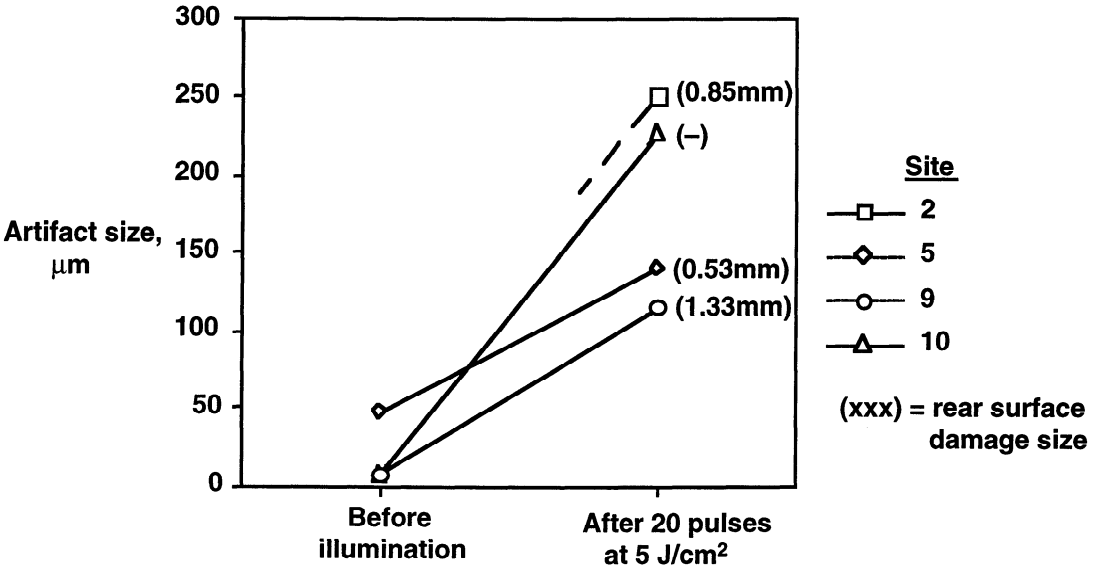

Figure 5. Diameters of pre-existing bulk inclusions and resulting bulk damage sites after 3ω illumination. Growth rates range from 5 to 12 μm/pulse. Corresponding rear surface damage sizes are also noted.

The range and average growth rate for the various types of surface-only damage are shown in Figure 7. Rear surface scratches had much higher growth rates (62.6 μm/pulse average) than either front-surface damage (5.2 μm/pulse) or other rear-surface damage (9.1 μm/pulse average). The high growth rates for rear surface scratches is consistent with the typical observation that optics tend to damage most severely on the rear surface. The lower growth rates for the no-visible-precursor rear damage sites may suggest that rear surface damage may not clearly dominate for higher quality, scratch-free, surfaces.

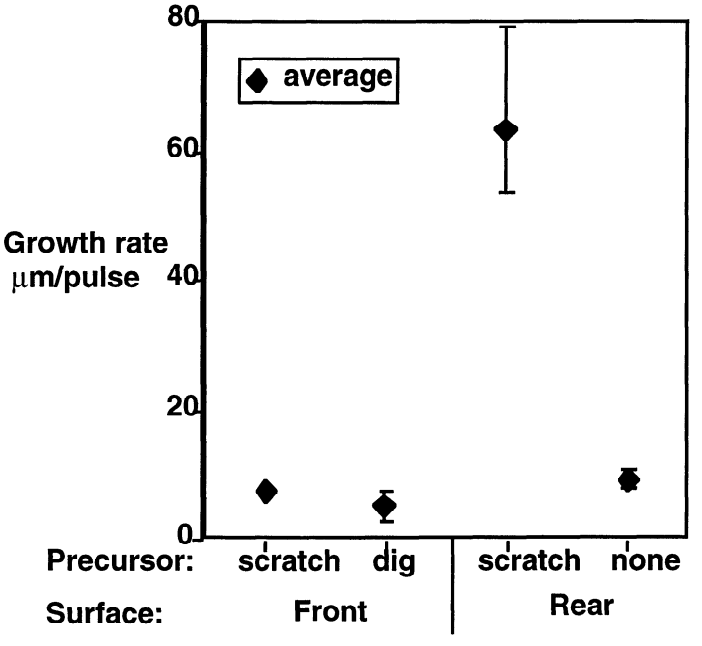

Figure 6. Surface damage growth rates calculated for damage due to twenty pulses at 5 J/cm^2, 3 ns on lens 02A.

Damage growth rates at bulk inclusions and corresponding rear surface damage sites are shown in figure 8. The average inclusion growth rate of 8.4 μm/pulse is quite similar to the growth rates for most of the surface damage at 3ω. There is significant spread in the growth rates for the inclusion-related rear surface damage, with some sites showing growth rates similar to that of rear surface scratches.

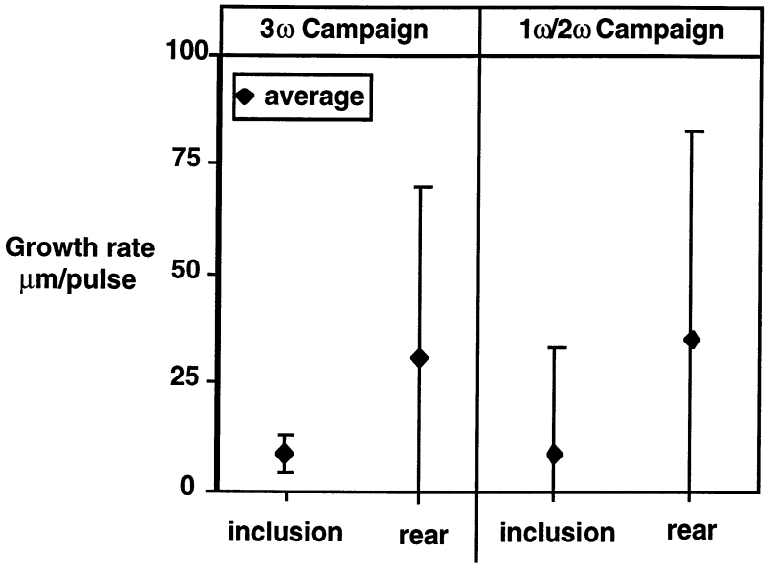

Figure 7. Growth rates for the inclusion-related bulk and rear-surface damage for both the 3ω and 1ω/2ω campaigns.

3.2 1ω/2ω illumination

Following the 47 pulse 1ω/2ω campaign, growth was observed on all fourteen of the damage sites previously examined using the long focal length microscope. No indication of initiation of new sites was indicated in the mega-pixel map. Growth rates for the 1ω/2ω campaign were calculated by simply dividing the change in size by the total number of pulses in the campaign. The growth rates are, therefore, average rates specific to this campaign rather than to a particular fluence, in contrast with the case for the 3ω tests. Several observations can be drawn from the 1ω/2ω surface damage data summarized in Figure 9. First we point out that the 1ω/2ω fluences used in this campaign would not have initiated damage by themselves. These fluences were capable, however, of increasing the size of damage initiated by 3ω illumination. This indicates that once damage is initiated, the lifetime of an optic is influenced by pulse energies and wavelengths that might have been considered benign from a damage initiation viewpoint. Second, the nominal growth rates are lower than for the 3ω campaign by approximately a factor of 10, suggesting a wavelength dependence of the growth rate. Third, for both the 1ω/2ω and 3ω campaigns the highest growth rates were observed for rear surface scratches.

Figure 8 shows the inclusion-related growth rates for both the 3ω and the 1ω/2ω campaigns. The average growth rate for the surface damage is higher than that of the bulk damage by about a factor of four in both campaigns. For the inclusion-related damage, however, the 1ω/2ω growth rate was not lower than the 3ω growth rate, in contrast with the case of purely surface-related damage (Figures 7 and 9).

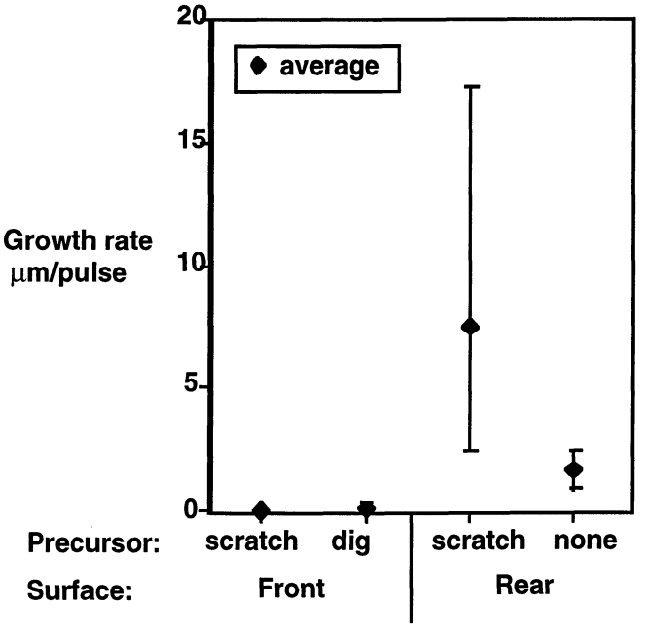

Figure 8. Surface damage growth rates calculated for damage due to 48 1ω/2ω pulses at maximum fluences of 4.8 J/cm^2 2ω, 5.7 J/cm^2 1ω , 1.5 ns on lens 02A. These growth rates are not associated with a particular fluence and are used for comparison of trends only.

4. CONCLUSIONS

The damage growth data obtained from the two Beamlet campaigns lead to several conclusions.

1. Rear surface scratches result in the highest growth rates for both 1ω/2ω and 3ω illumination.
2. For most bulk and surface damage sites the growth rate for 5 J/cm^2, 3ω, 3ns pulses is approximately 10 μm/pulse.
3. Otherwise benign 1ω/2ω fluences cause growth of damage sites initiated by 3ω pulses.

The data presented here will be used to qualify damage growth rate models derived from laboratory studies using smaller beams. Additional issues to be addressed include influence of pulselength, surface polishing procedure, and test environment (air vs. vacuum).

5. ACKNOWLEDGMENTS

Work performed under the auspices of the U.S. Department of Energy by Lawrence Livermore National Laboratory under Contract W-7405-ENG-48.

6. REFERENCES

1) S.C. Burkhart, K.R. Brading, P.M. Feru, M.R. Kozlowski, J.E. Murray, J.E. Rotherberg, B.M. Van Wonterghem, P.J. Wegner, T.L. Weiland, "High-fluence and High-Power 1.05 μm and 351 nm Performance Experiments on Beamlet," *this proceedings*, Monterey, 1998.

2) F. Genin, F., Salleo, A., unpublished results, LLNL, 1998.

3) M.D. Feit, F.Y. Genin, A.M. Rubenchik, L. Sheehan, M.R. Kozowski, J. Dijon, P. Garrec, "Statistical evaluation of damage risks in NIF and LMJ optics at 355 nm," *this proceedings*, Monterey, 1998.

4) D.W. Camp, M.R. Kozlowski, L.M. Sheehan, M.A. Nichols, M. Dovik, R.G. Raether, I.M. Thomas, "Subsurface damage and polishing compound affect the 355-nm laser damage threshold of fused silica surfaces," *Laser induced Damage in Optical Materials: 1997, SPIE*, **3244**, 356-364 (1998).

5) S. Schwartz, J.F. Kimmons, M.R. Kozlowski, L.M. Sheehan, C.J. Stolz, J.H. Campbell, "Vendor-based laser damage metrology equipment supporting the National Ignition Facility," *this proceedings*, Monterey, 1998.
6) F. Rainer, R.T. Jennings, J.F. Kimmons, S.M. Maricle, R.P. Mouser, S. Schwartz, C.L. Weinzapfel, "Development of practical damage-mapping and inspection systems," *this proceedings*, Monterey, 1998.
7) Feit, M.D., Rubenchik, A.M., "Laser intensity modulation by nonabsorbing defects," *Laser-induced Damage in Optical Materials, 1996 - SPIE*, **2966**, 475-480 (1997).

UCRL-JC-129721
PREPRINT

3ω Damage Threshold Evaluation of Final Optics Components using Beamlet Mule and Off-Line Testing

M. R. Kozlowski
S. Maricle
R. Mouser
S. Schwartz
P. Wegner
T. Weiland

This paper was prepared for submittal to the
Third Annual International Conference on
Solid State Lasers for Application (SSLA)
to Inertial Confinement Fusion (ICF)
Monterey, California
June 7-12, 1998

July 27, 1998

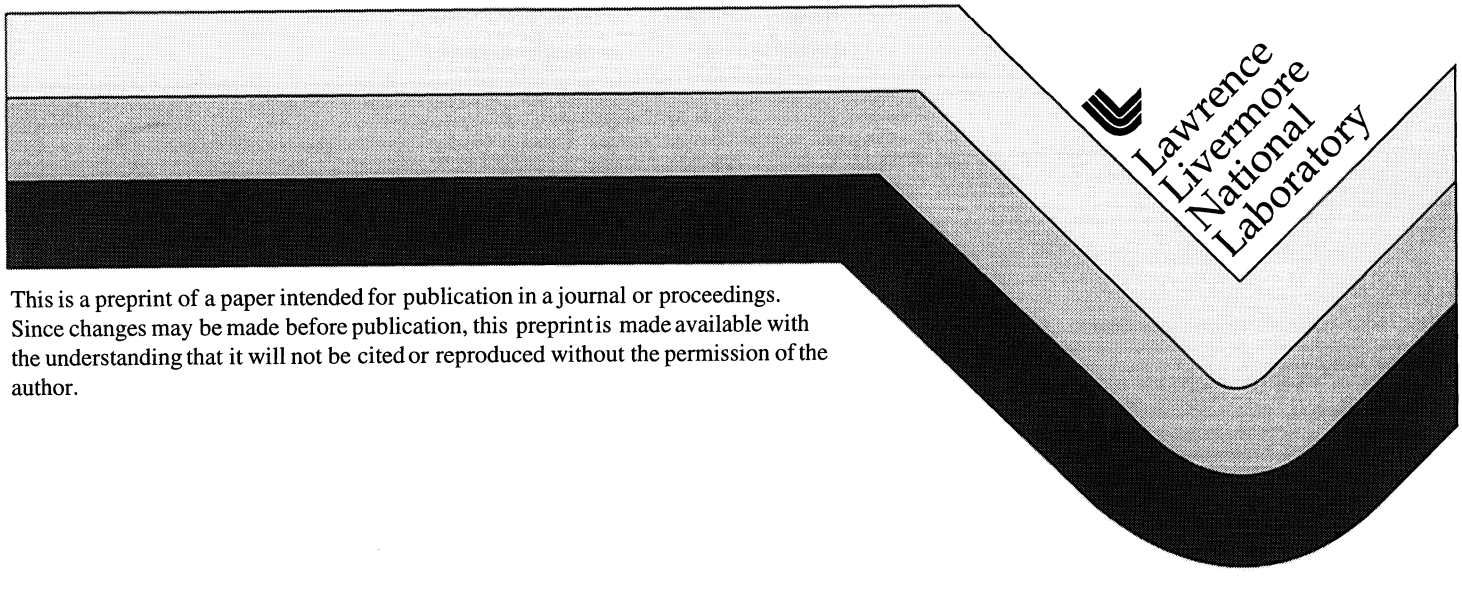

3ω Damage threshold evaluation of final optics components using Beamlet Mule and off-line testing

M.R. Kozlowski, S. Maricle, R. Mouser,
S. Schwartz, P. Wegner, T. Weiland
Lawrence Livermore National Laboratory
7000 East Avenue, Livermore, California, 94551

ABSTRACT

A statistics-based model is being developed to predict the laser-damage-limited lifetime of UV optical components on the NIF laser. In order to provide data for the model, laser damage experiments were performed on the Beamlet laser system at LLNL. An early prototype NIF focus lens was exposed to twenty 351 nm pulses at an average fluence of 5 J/cm^2, 3ns. Using a high resolution optic inspection system a total of 353 damage sites was detected within the 1160 cm^2 beam aperture. Through inspections of the lens before, after and, in some cases, during the campaign, pulse to pulse damage growth rates were measured for damage initiating both on the surface and at bulk inclusions. Growth rates as high as 79 μm/pulse (surface diameter) were observed for damage initiating at pre-existing scratches in the surface. For most damage sites on the optic, both surface and bulk, the damage growth rate was approximately 10μm/pulse.

The lens was also used in Beamlet for a subsequent 1053 μm/526 μm campaign. The 352 μm-initiated damage continued to grow during that campaign although at generally lower growth rates.

Key words: laser damage, fused silica, polishing, NIF, growth rate, defects, inclusions

1. INTRODUCTION

It is expected that under the aggressive illumination conditions of the National Ignition Facility (NIF) some laser-induced damage will occur in the fused silica optics transmitting UV laser light (351 nm or 3ω) to the target. The UV optics include the focus lens, diffractive optics plates (DOPs) and the debris shield. Combined with the KDP crystals used for frequency conversion, these optics make up the NIF final optics package. In order to evaluate the performance of final optics components, a testbed system, called the Mule, was added to the Beamlet laser system at LLNL.[1]

The goal of the experiments described here is to study the evolution of UV laser damage on a final focus lens within the Beamlet Mule. Information to be gained includes the density of damage sites on the optic and the rate of growth of the damage sites when exposed to additional laser pulses. This information will be used to develop a model for optics lifetime on the NIF laser.

Other studies have indicated that the diameter, D, of a laser damage site is fused silica grows as

$$D = N \cdot R(F) \qquad (1)$$

where N is the number of pulses and R is the growth rate in μm/pulse. R is a linear function of the fluence, F, in J/cm^2.[2] The growth rate R appears to depend on parameters such as the nature of the damage initiator, the environment of the optic (air or vacuum), and possibly the laser pulselength. In the present experiment R was to be determined at a fixed fluence for a NIF-scale focus lens (39 cm x 39 cm) in vacuum, the final optics environment in NIF.

Besides damage growth rate, the laser damage performance of an optic is determined by the density of damage initiation sites on an optic. In a paper by Feit, et al.[3] in these proceedings it is shown that the statistical nature of laser damage on surfaces can be modeled using the concepts of "extreme statistics." A methodology has been developed for predicting the density of damage sites on NIF-scale optics using data obtained by rastering an optic with 1 mm diameter gaussian laser beams. The purpose of the Beamlet Mule experiments is to provide data by which these statistical models can be evaluated.

2. DAMAGE TESTING AND OPTICS INSPECTION

2.1 Off-line testing results and inspection techniques

The tests discussed here involve two early prototype NIF reverse focus lenses 01A and 02A manufactured using ZrO_2 polishing processes. ZrO_2 polishing has been shown to result in improved laser damage performance as compared to the more common CeO_2 polishing processes.[4] Both lens was characterized before and after illumination using a Defect Mapping System (DMS). [6] This system uses fiber optic light bars to internally illuminate the optic through the four edges. A full aperture image of an optic is taken using a mega-pixel CCD camera. The system detects defects as small as 10μm over the full 40cm x 40cm optic. Due to blooming of the defects in the image, it is not possible to resolve the size or features or the individual defect/damage sites directly from the mega-pixel map. After identification of defects in the image, a long focal length microscope is used to photograph individual sites. For both lenses the majority of pre-existing surface defects were small scratches (<2mm long, <30μm wide) on the rear surface. These scratches were attributed to the use of ZrO_2 in the lens aspherization processes. Four bulk inclusions with diameters ranging from 7 to 48 μm were also observed in the lens.

Lens 01A was damage tested at 355 nm using a large-aperture raster scanning facility at LLNL (1mm diameter beam).[5] The lens was scanned at fluences ranging from 2.8 J/cm^2 to 14 J/cm^2, 3 ns, on a cumulative surface area of 80 cm^2. In those tests damage was observed at fluences as low as 2.8 J/cm^2. The damage occurred at pre-existing bulk and surface defects, as well as surface sites with no visible precursor (NVP). In those tests there was no obvious correlation indicated between damage size and precursor or fluence. Damage morphology studies using raster-scan techniques are complicated, however, by the "overlapping beam print" nature of the scanning process.

Based on the off-line tests of lens 01A, it was determined that in the Beamlet test lens 02A would be illuminated with 20 pulses at a fluence of 5 J/cm^2 average at 3ns. This fluence would provide a damage probability of <1% for 1mm^2 areas on the surface.

2.2 Beamlet Campaigns

Lens 02A was coated with a silica sol-gel anti-reflection coating before being installed in the Beamlet Mule. The Beamlet 3ω campaign included a six-pulse ramp from 0.8 to 4.3 J/cm^2 followed by twenty pulses at approximately 5 J/cm^2. The average beam modulation in the test was 1.31 to 1 (over 99.9% of area), resulting in peak fluences of approximately 7 J/cm^2. Figure 1 shows a plot of the peak and average fluences in the test. The lens was inspected inside the Mule twice during the campaign: after the first and twelfth 5 J/cm^2 pulses. Five damage sites were photographed during the inspections.

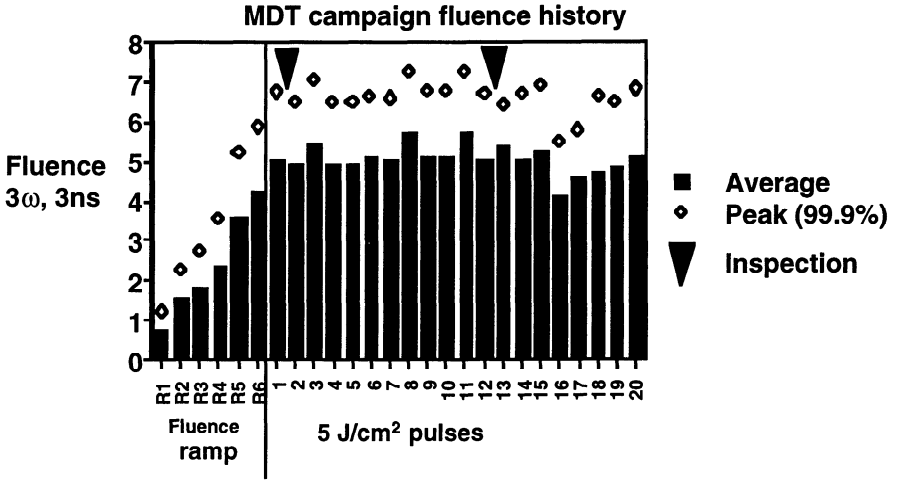

Figure 1. The 3ω campaign illuminated lens 02A with 20 pulses with an average fluence of 5.04 J/cm^2. Average modulation: 1.3.1 peak-to-average.

After the twenty shot 3ω campaign was completed the lens was removed from the Mule and mapped using the DMS system. Figure 2 shows the DMS map of the lens after the 3ω campaign. The mapping system identified 353 damage sites larger than 10 μm in diameter. As a result of camera blooming, the damage sites appear larger than they actually are. Fourteen damage sites representative of the 353 bulk and surface damage sites on the optic were further characterized using the long focal length microscope.

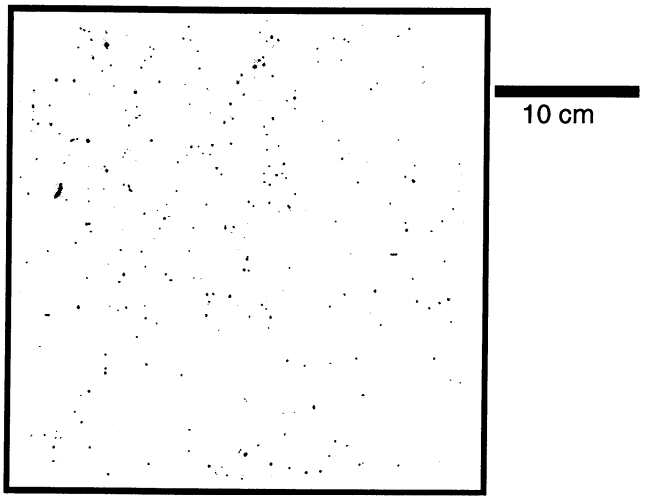

Figure 2. DMS map of lens 02A after twenty 5 J/cm^2 pulses. The map shows the location of 353 damage sites ranging in size from 10 μm to 2 mm within the 1160 cm^2 beam aperture

The lens was reinstalled on Beamlet for a series of low-fluence frequency doubling experiments. During that campaign the lens was exposed to 47 pulses of 1ω and 2ω illumination (1053 nm and 526 nm, respectively) with maximum intensities of 5.7 J/cm^2 and 4.3 J/cm^2 respectively at 1.5 ns. The mean 1ω and 2ω intensities were 2.2 J/cm^2 and 1.5 J/cm^2, respectively. Each of the fourteen sites measured after the 3ω campaign were again characterized after the 1ω/2ω campaign.

3. DAMAGE GROWTH RESULTS

3.1 3ω illumination

Damage size data obtained during the various lens inspections are shown graphically in figures 4-6. Figure 4 shows the data for the five sites characterized during the two intermediate inspections inside the Mule. The data for sites 1 and 2 support the assumption of a linear growth rate. Figure 5 shows the data for sites measured only before and after the 3ω campaign. In both figures 4 and 5 the steepest slopes (i.e. growth rates) are for preexisting scratches. The data does not indicate a clear correlation between precursor size and growth rate, consistent with the raster scan test result on lens 01A.

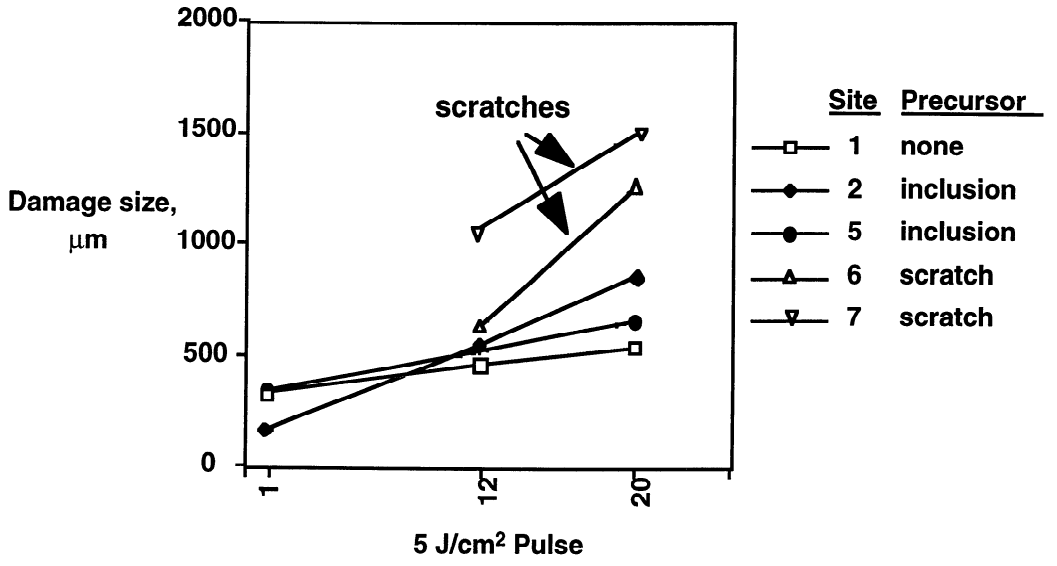

Figure 3. Damage size data for 5 rear surface sites measured during in-situ inspections. Growth rates range from 9 to 79 μm/pulse.

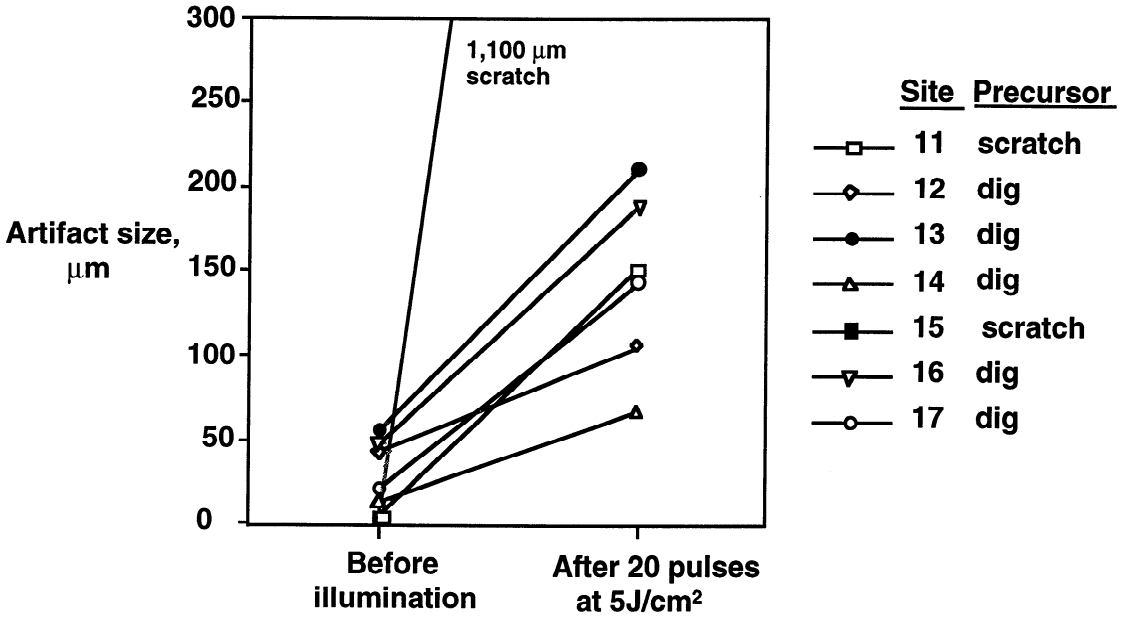

Figure 4. Sizes of damage associated with pre-existing surface defects. Growth rates range from 2.7 to 55 μm/pulse. All damage is front surface except for sites 13 and 15 (solid symbols).

Size data for damage at bulk inclusions is shown in figure 6. In figure 4, sites 2s and 5s are rear surface damage sites correlated with bulk inclusion damage. The rear surface damage is due to locally high fluences resulting from modulation of the beam by the bulk damage site.[7]

Damage growth rates were calculated from the defect/damage sizes shown in Figures 4-6 and assuming a linear growth rate. The growth rates were calculated counting only the shots at 5 J/cm^2, but not the initial six lower fluence pulses in the ramp. The influence of this simplification on the reported growth rates is small since most damage did not occur until the higher fluence shots. Damage growth rates for the 3ω campaign are summarized in figures 7 and 8, showing the dependence of the growth rate on damage precursor type (scratch, dig, inclusion, etc.) and location (bulk, input or output surface).

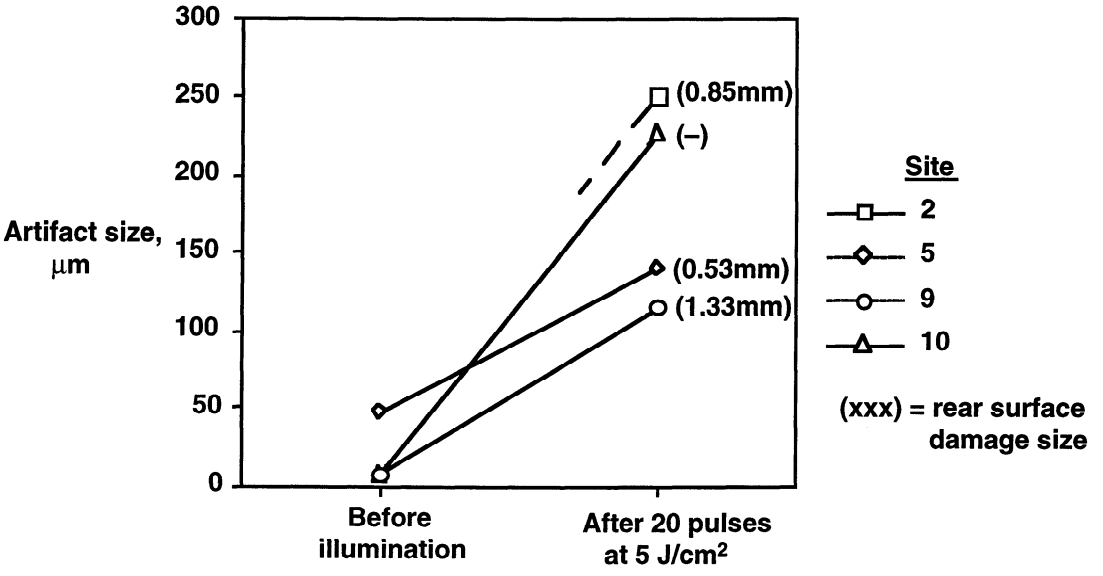

Figure 5. Diameters of pre-existing bulk inclusions and resulting bulk damage sites after 3ω illumination. Growth rates range from 5 to 12 μm/pulse. Corresponding rear surface damage sizes are also noted.

The range and average growth rate for the various types of surface-only damage are shown in Figure 7. Rear surface scratches had much higher growth rates (62.6 μm/pulse average) than either front-surface damage (5.2 μm/pulse) or other rear-surface damage (9.1 μm/pulse average). The high growth rates for rear surface scratches is consistent with the typical observation that optics tend to damage most severely on the rear surface. The lower growth rates for the no-visible-precursor rear damage sites may suggest that rear surface damage may not clearly dominate for higher quality, scratch-free, surfaces.

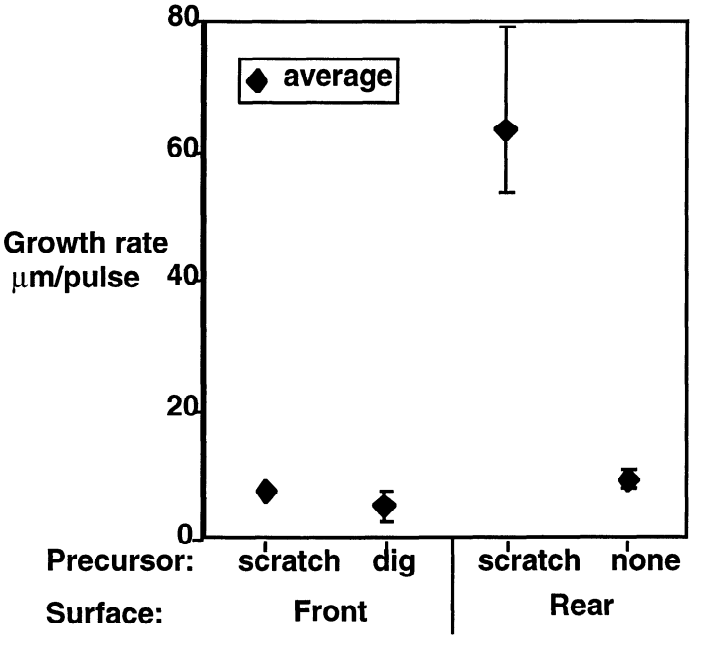

Figure 6. Surface damage growth rates calculated for damage due to twenty pulses at 5 J/cm^2, 3 ns on lens 02A.

Damage growth rates at bulk inclusions and corresponding rear surface damage sites are shown in figure 8. The average inclusion growth rate of 8.4 μm/pulse is quite similar to the growth rates for most of the surface damage at 3ω. There is significant spread in the growth rates for the inclusion-related rear surface damage, with some sites showing growth rates similar to that of rear surface scratches.

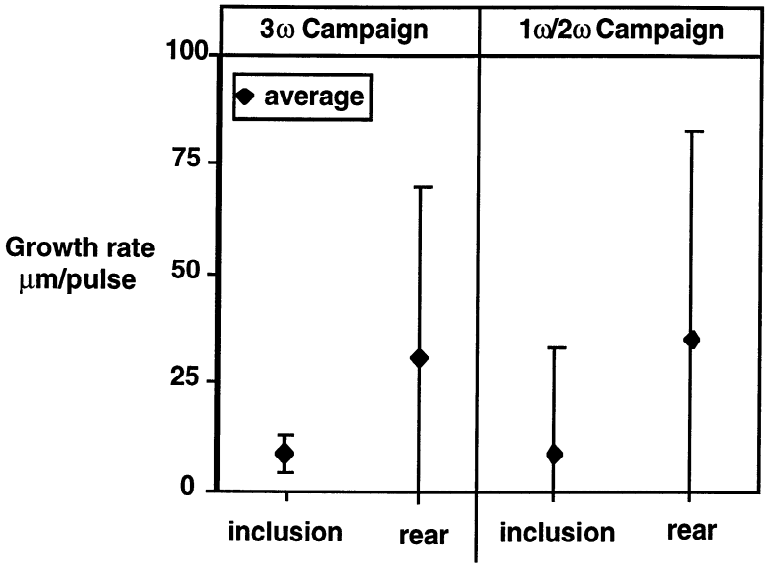

Figure 7. Growth rates for the inclusion-related bulk and rear-surface damage for both the 3ω and 1ω/2ω campaigns.

3.2 1ω/2ω illumination

Following the 47 pulse 1ω/2ω campaign, growth was observed on all fourteen of the damage sites previously examined using the long focal length microscope. No indication of initiation of new sites was indicated in the mega-pixel map. Growth rates for the 1ω/2ω campaign were calculated by simply dividing the change in size by the total number of pulses in the campaign. The growth rates are, therefore, average rates specific to this campaign rather than to a particular fluence, in contrast with the case for the 3ω tests. Several observations can be drawn from the 1ω/2ω surface damage data summarized in Figure 9. First we point out that the 1ω/2ω fluences used in this campaign would not have initiated damage by themselves. These fluences were capable, however, of increasing the size of damage initiated by 3ω illumination. This indicates that once damage is initiated, the lifetime of an optic is influenced by pulse energies and wavelengths that might have been considered benign from a damage initiation viewpoint. Second, the nominal growth rates are lower than for the 3ω campaign by approximately a factor of 10, suggesting a wavelength dependence of the growth rate. Third, for both the 1ω/2ω and 3ω campaigns the highest growth rates were observed for rear surface scratches.

Figure 8 shows the inclusion-related growth rates for both the 3ω and the 1ω/2ω campaigns. The average growth rate for the surface damage is higher than that of the bulk damage by about a factor of four in both campaigns. For the inclusion-related damage, however, the 1ω/2ω growth rate was not lower than the 3ω growth rate, in contrast with the case of purely surface-related damage (Figures 7 and 9).

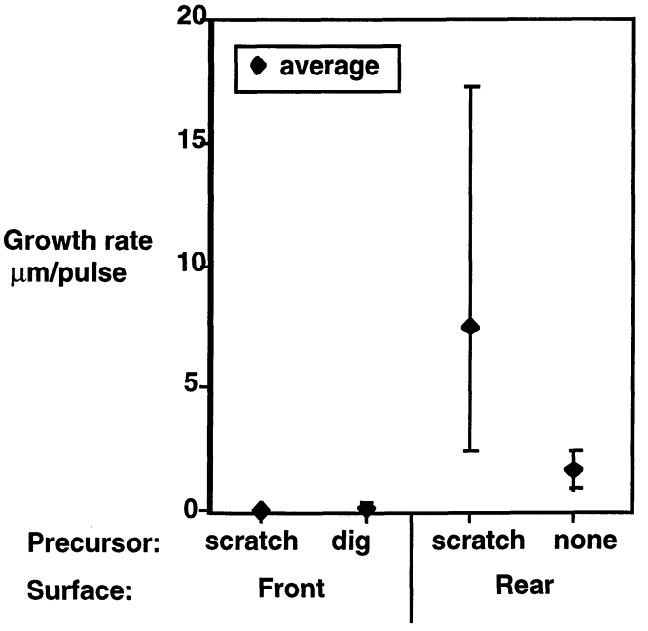

Figure 8. Surface damage growth rates calculated for damage due to 48 1ω/2ω pulses at maximum fluences of 4.8 J/cm^2 2ω, 5.7 J/cm^2 1ω , 1.5 ns on lens 02A. These growth rates are not associated with a particular fluence and are used for comparison of trends only.

4. CONCLUSIONS

The damage growth data obtained from the two Beamlet campaigns lead to several conclusions.

1. Rear surface scratches result in the highest growth rates for both 1ω/2ω and 3ω illumination.
2. For most bulk and surface damage sites the growth rate for 5 J/cm^2, 3ω, 3ns pulses is approximately 10 μm/pulse.
3. Otherwise benign 1ω/2ω fluences cause growth of damage sites initiated by 3ω pulses.

The data presented here will be used to qualify damage growth rate models derived from laboratory studies using smaller beams. Additional issues to be addressed include influence of pulselength, surface polishing procedure, and test environment (air vs. vacuum).

5. ACKNOWLEDGMENTS

Work performed under the auspices of the U.S. Department of Energy by Lawrence Livermore National Laboratory under Contract W-7405-ENG-48.

6. REFERENCES

1) S.C. Burkhart, K.R. Brading, P.M. Feru, M.R. Kozlowski, J.E. Murray, J.E. Rotherberg, B.M. Van Wonterghem, P.J. Wegner, T.L. Weiland, "High-fluence and High-Power 1.05 μm and 351 nm Performance Experiments on Beamlet," *this proceedings*, Monterey, 1998.

2) F. Genin, F., Salleo, A., unpublished results, LLNL, 1998.

3) M.D. Feit, F.Y. Genin, A.M. Rubenchik, L. Sheehan, M.R. Kozowski, J. Dijon, P. Garrec, "Statistical evaluation of damage risks in NIF and LMJ optics at 355 nm," *this proceedings*, Monterey, 1998.

4) D.W. Camp, M.R. Kozlowski, L.M. Sheehan, M.A. Nichols, M. Dovik, R.G. Raether, I.M. Thomas, "Subsurface damage and polishing compound affect the 355-nm laser damage threshold of fused silica surfaces," *Laser induced Damage in Optical Materials: 1997, SPIE*, **3244**, 356-364 (1998).

5) S. Schwartz, J.F. Kimmons, M.R. Kozlowski, L.M. Sheehan, C.J. Stolz, J.H. Campbell, "Vendor-based laser damage metrology equipment supporting the National Ignition Facility," *this proceedings*, Monterey, 1998.
6) F. Rainer, R.T. Jennings, J.F. Kimmons, S.M. Maricle, R.P. Mouser, S. Schwartz, C.L. Weinzapfel, "Development of practical damage-mapping and inspection systems," *this proceedings*, Monterey, 1998.
7) Feit, M.D., Rubenchik, A.M., "Laser intensity modulation by nonabsorbing defects," *Laser-induced Damage in Optical Materials, 1996 - SPIE*, **2966**, 475-480 (1997).